

ERRATUM: “LIGHT SCATTERING FROM EXOPLANET OCEANS AND ATMOSPHERES” (2010, *ApJ*, 723, 1168)

MICHAEL E. ZUGGER^{1,2}, JAMES F. KASTING^{2,3}, DARREN M. WILLIAMS^{2,4}, TIMOTHY J. KANE^{1,5}, AND C. RUSSELL PHILBRICK⁶

¹ Penn State University, Applied Research Laboratory, P.O. Box 30, State College, PA 16804, USA

² Center for Exoplanets and Habitable Worlds, The Pennsylvania State University, University Park, PA 16802, USA

³ Department of Geosciences, Penn State University, 443 Deike Bldg., University Park, PA 16802, USA

⁴ School of Science, Penn State Erie, The Behrend College, 4205 College Drive, Erie, PA 16563-0203, USA

⁵ Department of Electrical Engineering, Penn State University, Electrical Engineering East, University Park, PA 16802, USA

⁶ Physics Department, North Carolina State University, 432 Riddick Hall, Raleigh, NC 27695-8202, USA

Received 2011 May 17; published 2011 September 6

Online-only material: color figure

1. INTRODUCTION

In the published article (Zugger et al. 2010), we modeled orbital light curves from various hypothetical planet types in edge-on orbits as seen from Earth. The intent was to determine how orbital variations in brightness and polarization of terrestrial exoplanets could be used to determine characteristics of the planetary atmospheres and surfaces, in particular, to detect the presence of large oceans on the planet surface. Polarization fractions and relative flux are plotted against orbital longitude (OL), which is defined such that $OL = 0^\circ$ when the planet is in transit (new phase), $OL = 90^\circ$ or 270° when the planet is in quadrature, and $OL = 180^\circ$ when the planet is in secondary transit (full phase). Modeled planets have a homogeneous atmosphere and a single surface type.

After discovering an error in our original code, which affects the shape of some of the orbital light curves for ocean planets, we provide this erratum with the affected figures updated. Some values in Table 1 have also been changed slightly. The general results and conclusions of the paper are not affected, but the updated figures and table are provided here for completeness. We provide a brief discussion of the differences below. The figures affected are Figure 2 and Figures 6–12. The last two rows of Table 1 are also affected.

2. UPDATED FIGURES

Figure 2 compares the shapes of normalized flux (unpolarized) orbital light curves from three end-member planet types: an ocean planet with a thin atmosphere, a Lambertian planet, and a planet where atmospheric Rayleigh scattering dominates. The brightness peak near $OL = 30^\circ$ is distinctive of an ocean-covered planet (although not necessarily a water ocean). This figure differs from the original figure only in a slight decrease in relative brightness of the ocean planet near full phase.

Figure 6 shows the relative flux from the vertical and horizontal polarizations, the total flux, and the polarization fraction versus orbital longitude. Here, the only effect of the correction is to raise the polarization fraction curve slightly so that it more closely approximates the Fresnel analytical result.

Figure 7 shows the effect of wind-driven waves and sea foam on the polarization fraction. The correction brings the curves for 10 m s^{-1} and 14 m s^{-1} closer to the 5 m s^{-1} curve, indicating a reduced estimation of the effect of wind.

Figure 8 compares the current model results with those from Williams & Gaidos (2008) under the same conditions—an ocean planet with a thin atmosphere and sea surface roughness equivalent to 10 m s^{-1} wind on Earth. The effect of the correction is to slightly increase the polarization fraction in the current model so that it moves away from the Williams & Gaidos (2008) result.

In Figure 9, we compare the polarization fraction for a water planet with a thin atmosphere and a water planet with a 1 atm Rayleigh scattering atmosphere against the Fresnel analytical curve. In the corrected version, the curve for the planet with atmospheric Rayleigh

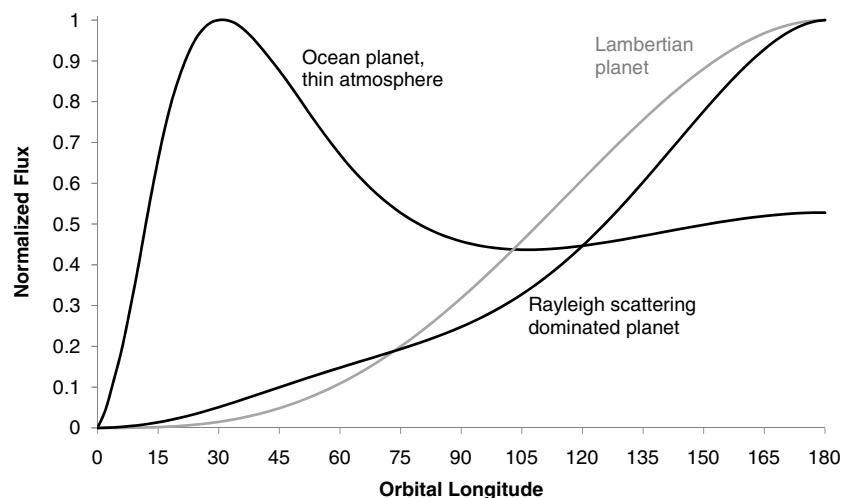


Figure 2. Normalized total light curves for end-member planets. The peak near $OL=30^\circ$ is indicative of an ocean surface (although not necessarily water).

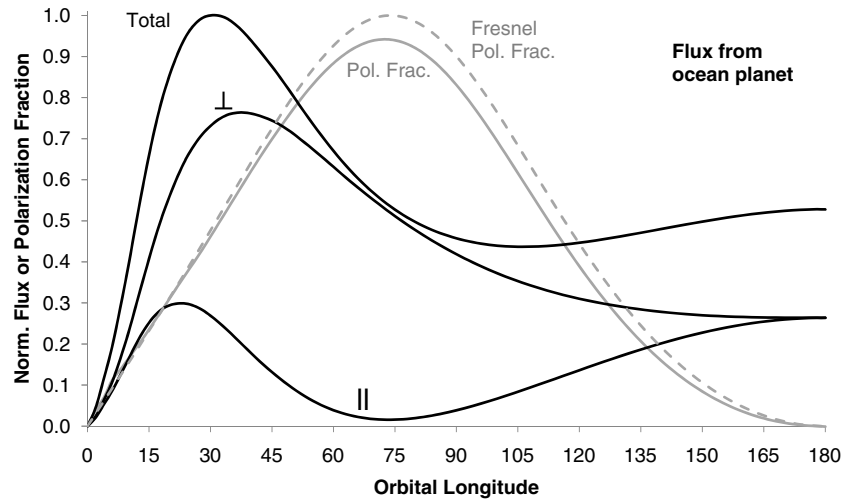


Figure 6. Polarized light curves (black) and polarization fraction (gray) for planet with calm ocean and thin atmosphere, wavelength range 500–1000 nm. The Fresnel curve for light reflecting from a flat air/water boundary is shown for comparison. The model departs from Fresnel theory primarily because of scattering from within the water at the shorter wavelengths.

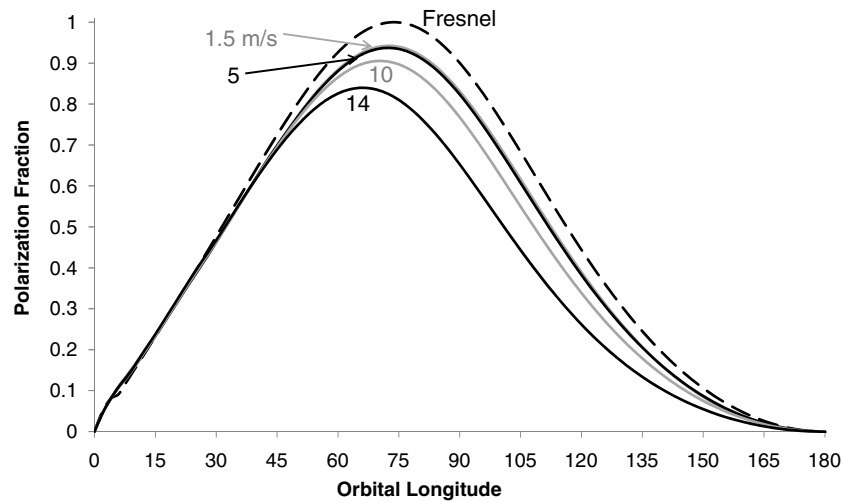


Figure 7. Polarization fraction for ocean planets vs. wind speed (no absorption, no aerosols, no Rayleigh scattering). For the TPF-C wavelength range 500–1000 nm, at wind speeds at and below 5 m s^{-1} , polarization fraction is limited by scattering within the water; at higher wind speeds, sea foam is the primary limiting factor on polarization fraction.

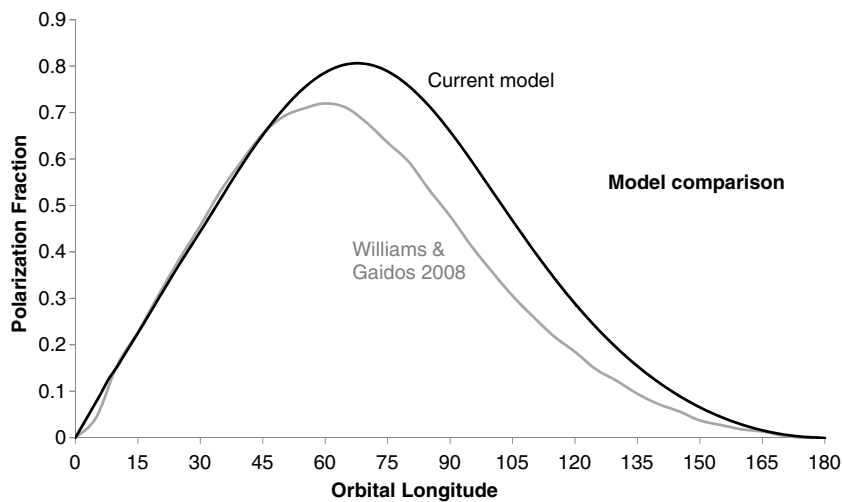


Figure 8. Comparison of polarization fraction results from Williams & Gaidos (2008) Figure 7(b) and the current model with a thin atmosphere and waves equivalent to Earth oceans with a surface wind of 10 m s^{-1} . The primary differences between the ocean models are that the current model uses a slightly different parameterization of wind-generated sea foam, uses Lambertian rather than isotropic scattering from sea foam, and includes scattering from within the water column. (Current model run with wavelength range 500–1000 nm; Williams & Gaidos 2008 model is wavelength independent.)

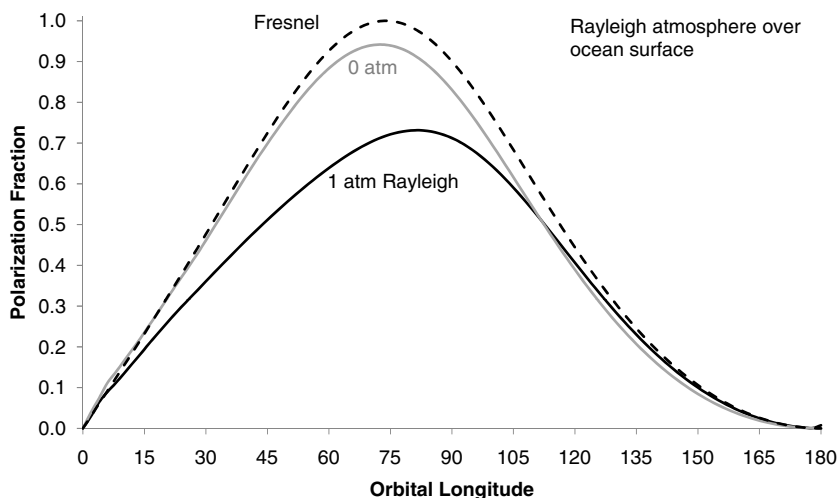


Figure 9. Polarization ratio for ocean planets with Earth-like atmospheric Rayleigh scattering or no atmospheric Rayleigh scattering for the TPF waveband 500–1000 nm. Both atmospheric and in-water scattering are significant at the shorter end of this band. Wind is calm (1.5 m s^{-1}), and absorption and aerosols are neglected.

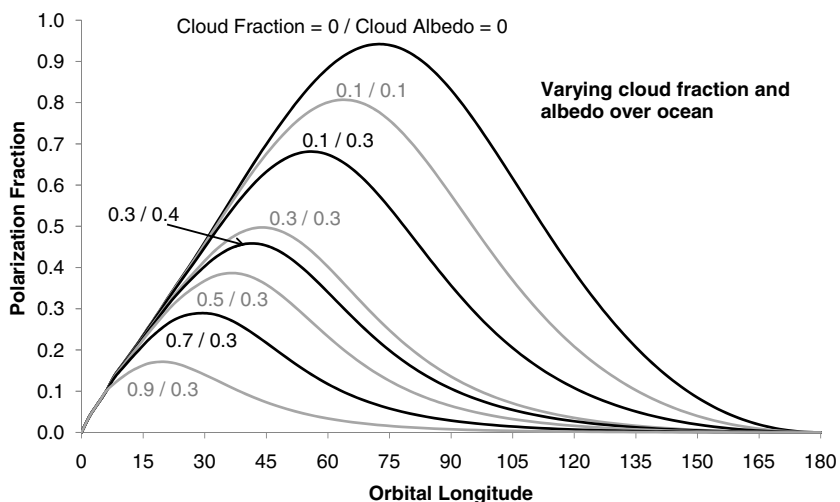


Figure 10. Polarization fraction for ocean planet with varying cloud fraction and cloud albedo. As with clouds and a Rayleigh atmosphere (Figure 5), unpolarized scattering from clouds dilutes polarization signatures. (Wavelength range 500–1000 nm.)

scattering and an ocean surface has a lower polarization fraction, and the peak is moved to lower OL. The polarization fraction for the ocean under a thin atmosphere increases slightly (this curve is identical to the polarization fraction curve in Figure 2).

Figure 10 shows the effect of various cloud fractions and cloud albedos on the polarization fraction. In the corrected figures, all polarization fractions increase slightly.

Figure 11 graphs polarization fractions for a number of water Earth planets, with a calm ocean surface (1.5 m s^{-1} wind), Earth-like atmospheric absorption and Rayleigh scattering, and several levels of aerosols parameterized by visibility at 550 nm. The magnitude of the polarization fractions of these water Earths decreases in the corrected versions, but the corrected versions are otherwise similar to the original figures.

In Figure 12, we graph the peak polarization fraction of each case previously discussed on a single figure, therefore converting each previous polarization fraction curve into a single data point on this figure. This allows us to see trends as parameters vary. The correction affects the curves representing ocean planets, that is, the green, blue, violet, and gray curves. The black (+) and red (diamonds) curves, which represent dry planet types, are not affected.

The green curve (circles) represents ocean planets with thin atmospheres and increasing clouds. The change in this curve is almost undetectable. The violet curve (triangles) shows the impact of increasing wind-driven waves and sea foam on the polarization fraction. As we saw in Figure 11, the effects of increasing wind are diminished in the corrected model, so the length of the violet curve is reduced. The violet “waves” curve also now falls almost directly on the green “cloud” curve.

The largest change in Figure 12 is the placement of the point representing an Earth-like absorption and Rayleigh scattering atmosphere (without aerosols) over a calm ocean. This point is the endpoint of both the blue and gray curves; the blue curve (squares) represents an increasingly thick Rayleigh scattering atmosphere over a calm ocean, and the gray curve (asterisks) represents planets with Earth-like absorption and Rayleigh scattering over a calm ocean, with increasingly thick aerosols. The intersection point of the two curves remains at about the same orbital longitude ($\sim 82^\circ$), but the polarization fraction at this point decreases from about 0.96

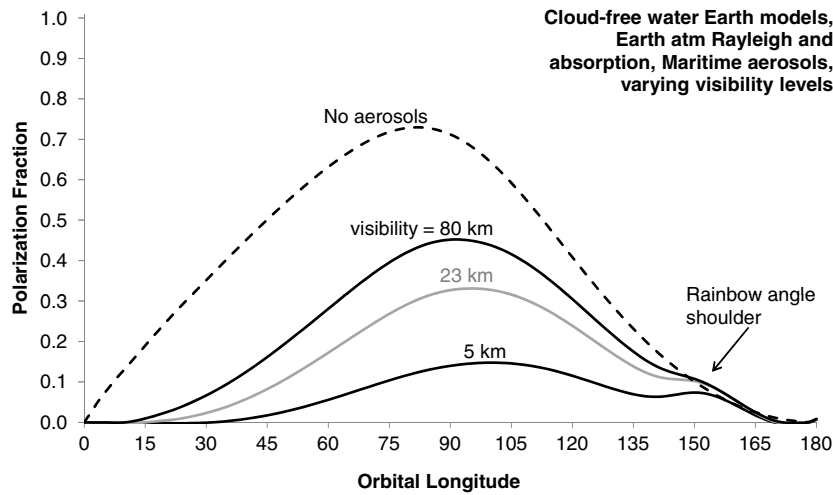


Figure 11. Water Earth models with varying aerosols. Aerosol versions show large reduction in the peak polarization, even for relatively clear 23 km visibility; also exhibit a shoulder near $OL = 140^\circ$ due to rainbow angle peak. All three curves assume an ocean planet with Earth atmosphere Rayleigh and absorption, and a surface wind speed of 1.5 m s^{-1} . (Wavelength range 500–1000 nm.)

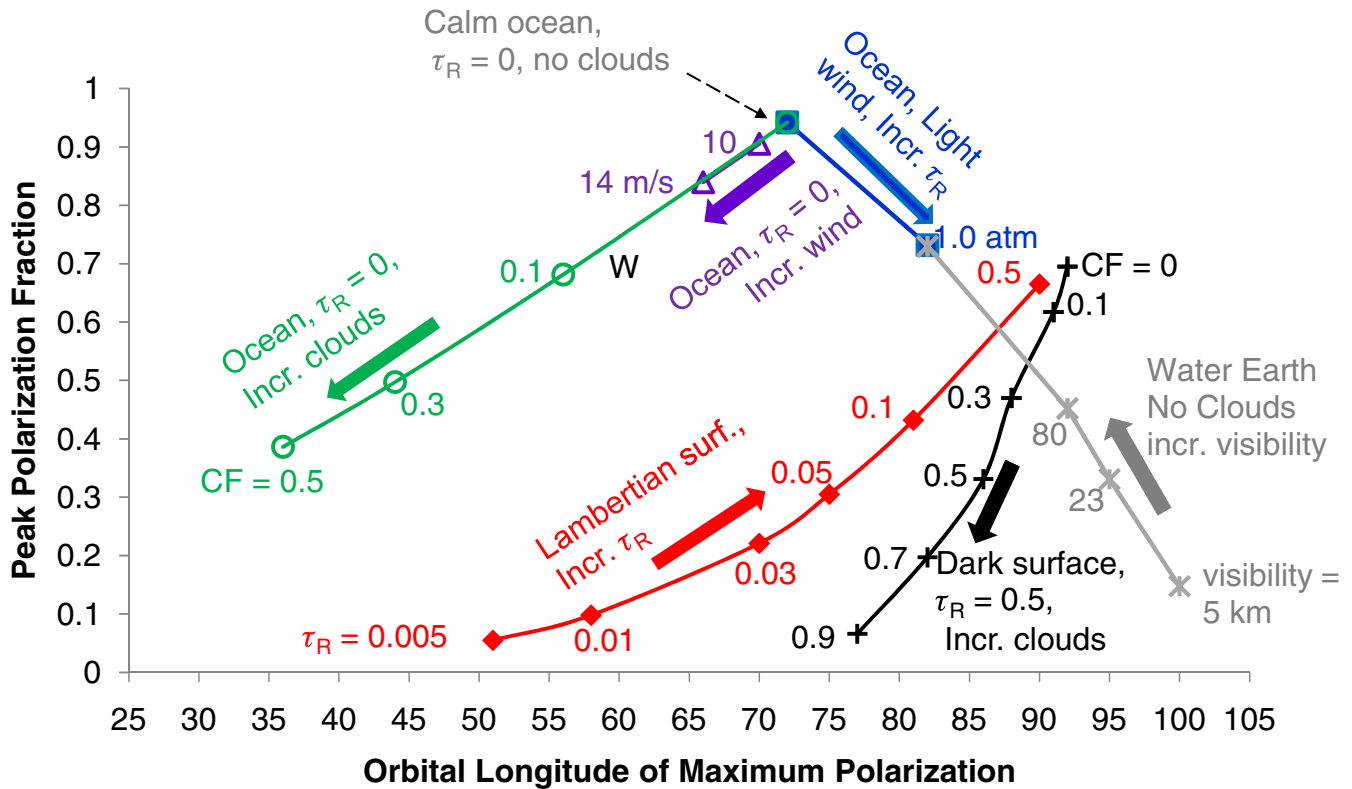


Figure 12. Summary of polarization fraction results for various planet types over the TPF waveband (500–1000 nm). Green curve (circles) represents an ocean planet with increasing clouds; violet curve (triangles) models an ocean planet with increasing surface wind; blue curve (squares) represents an ocean planet with increasing Rayleigh atmospheric depth. Red curve (diamonds) represents Lambertian surface with increasingly thick Rayleigh scattering atmosphere; black curve (+) represents a thick Rayleigh atmosphere over a dark surface, with increasing clouds W shows Williams & Gaidos 2008 result for an ocean planet with 10 m s^{-1} winds. Water Earths are shown by the gray curve (*) and include 1.5 m s^{-1} wind, Earth Rayleigh scattering, and US 1962 absorption model.

(A color version of this figure is available in the online journal.)

to about 0.73 in the corrected version. As a result, the blue curve now slopes down, indicating reduced polarization fraction with increasingly thick Rayleigh atmosphere. Also, the gray curve representing water Earths with varying levels of aerosols has lower polarization fractions throughout the curve. (The gray “water Earth” curve includes atmospheric absorption, and the blue “Rayleigh over ocean” curve does not, but the difference in polarization fraction due to Earth-like atmospheric absorption is less than 1% in this waveband.)

Table 1
Contrast Ratios for Lambertian and Ocean Planets with Thin Atmospheres

Surface	$C(90^\circ)$ Rel. to Lamb.	$C(180^\circ)$ Rel. to 2% Mirror	Comments
<i>Lambertian; $A_{bond} = 0.3$</i>	<i>1.000</i>	...	<i>From Sobolev (1975)/TPF report</i>
Cloud Lambertian, $A = 0.3$	0.997	...	Cloud albedo = 0.3, cloud fraction = 1
Surface Lambertian, $\rho = 0.3$	0.998	...	Surface $\rho = 0.3$, cloud fraction = 0
<i>Spherical mirror; $\rho = 0.02$</i>	...	<i>1.00</i>	<i>From Tousey (1957)</i>
Ocean 1.5 m s^{-1} , 900–1000 nm	0.078	1.05	Rayleigh reduced using longer wavelengths
Ocean 1.5 m s^{-1} , 500–1000 nm	0.083	1.25	Significant Rayleigh scattering within water

Note. Rows in bold italics show results from analytical calculations for comparison.

3. UPDATED TABLE

Table 1 also required a minor update. The values of contrast ratios for the ocean planets (bottom two rows) have been reduced by about 9% (bottom row) and 1% (second to bottom row), bringing the model into closer agreement with the Fresnel analytical result.

REFERENCES

- Tousey, R. 1957, *J. Opt. Soc. Am.*, 47, 261
 Williams, D. M., & Gaidos, E. 2008, *Icarus*, 195, 927
 Zuger, M. E., Kasting, J. F., Williams, D. M., Kane, T. J., & Philbrick, C. R. 2010, *ApJ*, 723, 1168